Hurricane Risk of Solar Generation in the United States

Luis Ceferino[1,2](*), Ning Lin[3,4]

[1]Civil and Urban Engineering Department, New York University
[2]Center for Urban Science and Progress, New York University
[3]Civil and Environmental Engineering, Princeton University
[4]The Andlinger Center for Energy and the Environment, Princeton University

(*) Email: ceferino@nyu.edu

Abstract

Projections indicate that solar energy will constitute 55% of total electricity capacity by 2050 in the US. Despite solar energy's growing importance, few studies have analyzed the risks of country-wide deployments of solar infrastructure due to extreme weather events such as hurricanes. This paper presents a probabilistic framework to evaluate the performance of solar infrastructure to generate energy during hurricanes, which often cause significant outages in the US. Our novel framework integrates recent data-driven models that capture two critical and compounding factors: transient cloud conditions that decrease irradiance and high winds that can cause permanent panel damage. We apply the framework to the 2694 counties in the 38 Central and Eastern US states to elucidate the risk landscape of solar generation during hurricanes. Our results show that hurricane impacts are significant, compounding, and strikingly disproportional in the US. We show that in Florida and Louisiana, clouds rapidly reduce solar generation to 32% and 65%, respectively, of their normal levels with a return period of 100 years. Our results also show that damage to panels can induce more acute and permanent energy losses a few days after landfall, especially in rarer storms, e.g., causing 80% more losses than hurricane clouds two days after landfall for 200-year events.

Synopsis: A new methodology to model solar generation during hurricanes shows substantial regional variability in the environmental risk landscape of solar infrastructure in the US.

Keywords: solar panels; energy resilience; hurricane risk; solar irradiance; wind damage.

This paper has been submitted to the journal of Environmental Science & Technology for publication.

Introduction

Ensuring continuous electricity delivery is key to supporting communities in responding and recovering from extreme natural events. Nevertheless, the grid is far from resilient. Hurricane Maria in 2017, for example, caused one of the longest and largest power outages in modern United States (US), which left half of Puerto Rico without power for at least four months.[1] Last year, Hurricane Ida damaged 30,000 utility poles, leaving 1.2 million customers without power across eight states[2], ranking as the costliest disaster in the world in 2021.[3]

Governments are investing aggressively in upgrading the grid to enhance resilience. Through the Bipartisan Infrastructure Law, the US Department of Energy (DOE) will provide USD 2.3 billion over the next five years to strengthen US power systems against extreme weather.[4] Furthermore, through the Bipartisan Infrastructure Law and the 2022 Energy Act, the US will invest even more ambitiously (USD 62 billion) in accelerating renewable adoption, including solar energy, to achieve net-zero electricity by 2035 and become a net-zero economy by 2050.[5] Motivated by the need to plan for these large-scale investments holistically, this paper studies the large-scale risk landscape of solar generation to hurricanes across the entire Central and Eastern US.

We focus on solar panels because the US Energy Information Administration (EIA) projects them to constitute 55% of total electricity capacity by 2050[6] and also because they have a high potential to increase resilience when deployed as a distributed energy resource. In fact, the USD 2.3-billion investments to modernize the grid include utilizing distributed energy resources as a key pillar to enhance resilience[4]. For example, rooftop solar panels and behind-the-meter batteries together can provide continuous energy to communities in an outage in the main grid.[7,8] Despite these opportunities, little is known about the ability of panels to generate electricity during hurricanes.

Extensive energy system models can assess disruptions in power systems,[9–11] enabling the design of strategies for risk mitigation (e.g., grid hardening) or emergency response (e.g., grid operations and repairs).[12–19] Nevertheless, these studies build on critical assumptions about electricity generation during extreme weather events, especially for solar energy during hurricanes. Many studies focus on damage to the distribution lines, not considering that extreme weather events also damage infrastructure for energy generation.[15,17–19] Recent observations have shown extensive wind-induced failures in rooftop and ground-mounted panels after Hurricane Irma, Maria, and Dorian in 2017 and 2019.[20–22] Other system models assume that energy sources remain constant during extreme weather events, neglecting transient environmental effects.[12–14,16,23] Yet, hurricanes bring optically-thick clouds that can absorb and reflect light and thus decrease generation drastically, e.g., to a fifth,[24] during a hurricane emergency.[25]

Current system models cannot capture these effects because no existing quantitative methods take them into account. These effects are complex as they are compounding and dynamic, i.e., they co-occur with conditions that vary rapidly over a storm's lifespans. DOE, energy regulators, and utility companies must account for these acute effects to assess the risk of solar generation losses and strategize a risk-informed response to outages and an effective deployment of solar energy for grid resilience.

To address this research gap, we present a probabilistic framework to quantify solar generation during hurricanes. This framework integrates recently developed data-driven models to capture the stochasticity in panels' structural performance and the intermittency of solar generation during hurricanes. We first apply the framework to study Miami-Dade, Florida, which faces high hurricane hazards[26,27] and large-scale hurricane-triggered outages.[28] Then, we extend the study to the 38 Central and Eastern US states at the county level to elucidate the risk landscape of solar generation. We reveal considerable variability in solar generation risks, highlighting where and when wind-induced panel failures and cloud-driven irradiance reduction are critical. Performing energy system studies to assess the implications of these energy losses on power delivery falls outside this paper's scope. Instead, we apply the proposed methodology to the US to create risk

maps of solar generation to help inform the response of utility operators during hurricanes and long-term investments in solar panels for grid resilience.

Materials and Methods

Compounding solar energy losses due to storms. We assess the time series of solar generation during hurricanes (Figure 1). Consider that P is the solar power generated during a storm and E is the total harvested energy until time t_f in the hurricane emergency. Thus,

$$E = \int_0^{t_f} P dt \tag{1}$$

If $\bar{E}$ is the counterfactual energy, i.e., the harvested energy that would have been collected at the same site and time in the absence of the hurricane, then

$$\bar{E} = E + \Delta E_c + \Delta E_d \tag{2}$$

where ΔE_c and ΔE_d are the energy losses due to could conditions and damage to the panels, respectively. Power generation is first affected by the cloud conditions brought by hurricanes[25], reducing the irradiance that reaches the panel according to hurricane intensity and proximity. When the hurricane leaves and it is at a sufficient distance away from the site, P will bounce back to normal levels. Thus, ΔE_c is transient. In contrast, if wind conditions are high enough, the panel will be damaged and remain unfunctional, driving power generation P to be permanently 0, starting at $t = t_d$, until the panel is repaired or replaced.[29] Thus, ΔE_d grows indefinitely, and the cumulative electricity generation E will become flat at $t = t_d$ until the panel is functional again. If there is no failure, ΔE_d will always be 0.

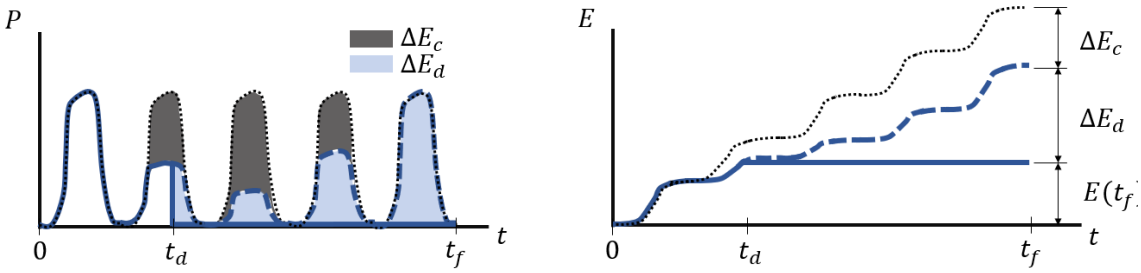

Figure 1. *Conceptual illustration of solar generation losses during hurricanes.* ***Left:*** *Instantaneous solar power generation.* ***Right:*** *Cumulative solar energy. The dashed blue line shows solar power and accumulated energy in a non-damaged solar panel during five days, i.e., from $t = 0$ to $t = t_f$. The dotted black lines show the counterfactual scenario, energy in the absence of the hurricane, highlighting the reduction in losses from hurricane cloud conditions ΔE_c – area in black in left figure and difference between ordinates in right figure. The solid blue line shows the generation and power for a panel the is damaged at $t = t_d$ due to high hurricane winds. The panel is unable to generate energy after $t = t_d$, generating additional energy losses ΔE_d – area in blue in left figure and difference between ordinates in right figure. Notice that generation will bounce back to normal levels as soon as the hurricane leaves if the panel is undamaged. If the panel is damaged, generation will be 0 after $t = t_d$ until it is repaired or replaced. Notice this conceptualization is valid for either small residential rooftop panel arrays or large ground-mounted arrays for utility companies.*

To assess the relative effect of these two factors on the total solar generation, we use two multiplicative factors to characterize solar generation during hurricanes

$$E = \frac{\bar{E}}{A_c A_d} \tag{3}$$

where A_c is a reduction factor that accounts for the energy losses due to the optically thick clouds reducing irradiance and is given by

$$A_c = \frac{\bar{E}}{\bar{E} - \Delta E_c} \tag{4}$$

and A_d is the reduction factor that accounts for the energy losses due to failures in the solar panel structural system and is given by

$$A_d = \frac{\bar{E} - \Delta E_c}{E} \tag{5}$$

Framework for simulating time-series of solar generation during storms. To evaluate these compounding effects, we model solar generation during storms in four stages (Figure 2). We based our assessment on ~50,0000 Monte Carlo simulations to capture the spatiotemporal complexities in the factors affecting generation. We first used simulations of landfalling synthetic hurricanes representative of the current climate in the Atlantic Basin[30]. These simulations of synthetic hurricanes track the maximum wind (and thus category C), storm size, and location of the hurricane's center, which enables the computation of its distance d to any site. This information is modeled at a fine temporal resolution of 2 hours, critical to capture intra-day variations of solar irradiance and rapid wind intensifications that can damage panels. In the second stage, we assess solar irradiance during hurricanes (I^h) using a recently developed mixed-regression model.[25] To capture the physics of irradiance decay with hurricanes, this model estimates irradiance decay as a function of hurricane category C and distance d normalized by storm size. In the third stage, solar panel functionality F (1 if there is no structural damage and 0 otherwise) and time-to-damage t_d are estimated stochastically. To account for these impacts on the panels' structural system, we use a study[29] that linked the likelihood of panel damage to varying winds (W) in hurricanes. We further detail stage 1, 2, and 3's models in the following subsections. In the fourth stage, we use I^h, F, and t_d to compute the synthetic time-series of instantaneous solar generation P and cumulative energy E.

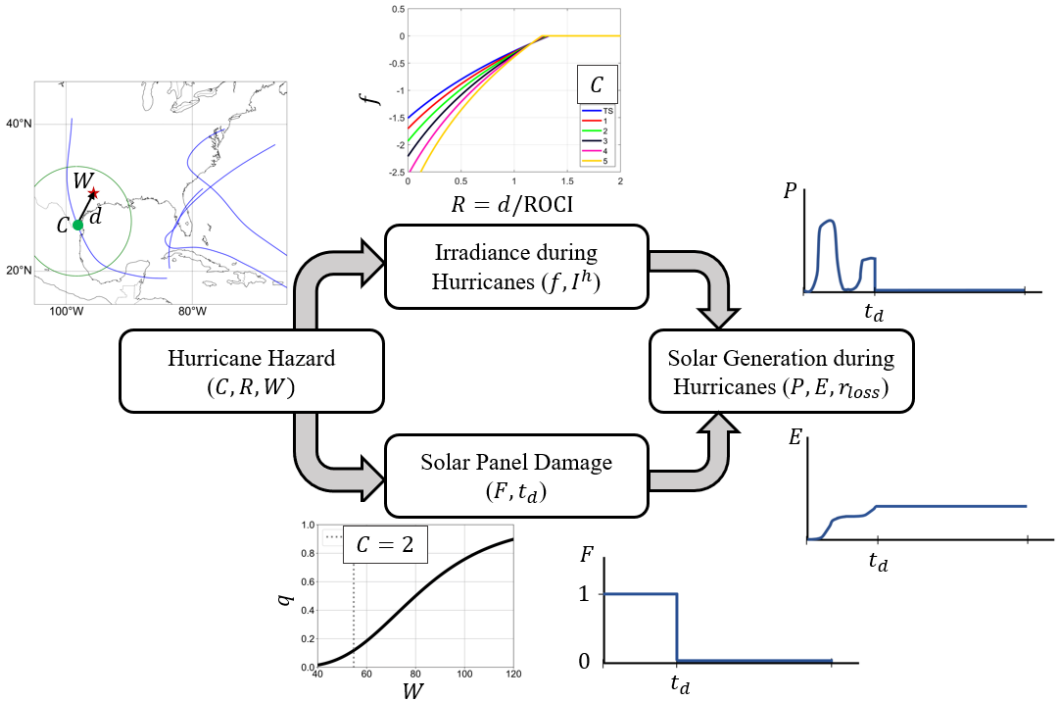

Figure 2. *Overview of proposed probabilistic framework to estimate the times series of solar generation during hurricanes. The analysis builds on the probabilistic modeling of hurricane hazards, solar damage due to high winds, and irradiance decays under hurricane cloud conditions to estimate the resulting solar generation.*

For a panel, with efficiency η (the ratio of energy that is converted into electricity form the solar energy reaching the panel) and area a, the instantaneous solar generation is

$$P = FI_h a\eta \tag{6}$$

If we isolate the effect of hurricane clouds (not considering panel failure), then $F = 1$ and

$$P = I_h a\eta \tag{7}$$

Additionally, in regular conditions,

$$\bar{P} = Ia\eta \tag{8}$$

where I is irradiance in the absence of a hurricane. Thus,

$$\Delta E_c = a\eta \int_0^{t_f} (I - I_h)dt \tag{9}$$

We then estimate our metrics for compounding effects reducing solar generation through the factors A_c and A_d. From Equation (4),

$$A_c = \frac{a\eta \int_0^{t_f} Idt}{a\eta \int_0^{t_f} Idt - a\eta \int_0^{t_f} (I - I^h)\, dt} = \frac{\int_0^{t_f} I\, dt}{\int_{t_0}^{t_f} I^h\, dt} \tag{10}$$

Similarly, from Equation (5),

$$A_d = \frac{a\eta \int_0^{t_f} Idt - a\eta \int_0^{t_f} (I - I^h)\, dt}{a\eta \int_0^{t_f} FI^h dt} = \frac{\int_0^{t_f} I^h dt}{\int_0^{t_f} FI^h dt} = \frac{\int_0^{t_f} I^h dt}{\int_0^{\min(t_d, t_f)} I^h dt} \tag{11}$$

Limiting behavior of compounding factors. Using L' Hospital's rule for the limiting behavior of A_c,

$$\lim_{t_f \to \infty} A_c = \frac{\int_0^{t_f} I\, dt}{\int_{t_0}^{t_f} I^h\, dt} = \lim_{t_f \to \infty} \frac{I}{I_h} \tag{12}$$

Because the hurricane eventually leaves or gets dissipated,

$$\lim_{t_f \to \infty} I_h = \lim_{t_f \to \infty} I \tag{13}$$

Thus,

$$\lim_{t_f \to \infty} A_c = 1 \tag{14}$$

In the case of A_d, if the panel does not fail, then $F = 1$, and $t_d = \infty$. Thus,

$$A_d = \frac{\int_0^{t_f} I^h dt}{\int_0^{t_f} I^h dt} = 1 \tag{15}$$

If the panel fails, $t_d < \infty$ and

$$\lim_{t_f \to \infty} A_d = \frac{\lim_{t_f \to \infty} \int_0^{t_f} I^h dt}{\int_0^{t_d} I^h dt} = \infty \tag{16}$$

Solar Irradiance during storms. I^h is the irradiance, e.g., Global Horizontal Irradiance, during hurricane conditions and can be estimated as

$$I^h = I e^{f(R,C)} \tag{17}$$

where I is irradiance under normal conditions, i.e., without a hurricane, at the time and location of interest. $f(R, C)$ is an irradiance decay equation as a function of the normalized proximity from the site to the hurricane center R and hurricane intensity C. This irradiance model was recently calibrated to ~0.75 M data points[25] from the 20-years of intense storm activity archived in the Atlantic hurricane dataset (HURDAT2)[31] and high-resolution spatiotemporal dataset of Global Horizontal Irradiance (GHI) from the National Renewable Energy Laboratory (NREL)[32]. Notice that R and C are highly variable in time, thus I^h is highly dynamic. Furthermore, I^h is stochastic as I is also random. Equation (17) implies that if I is modeled with a lognormal distribution, I^h is also lognormally distributed, with a logarithmic mean that is reduced by the factor $f(R, C)$. Empirically, this factor can be assessed as[25]

$$f = \begin{cases} (0.0965C + 1.97) ln\left(\dfrac{R + (-0.126C + 1.15)}{2.48 - 0.139C}\right) & \dfrac{R + (1.15 - 0.126C)}{2.48 - 0.139C} \leq 1 \\ 1 & \dfrac{R + (1.15 - 0.126C)}{2.48 - 0.139C} > 1 \end{cases} \tag{18}$$

where C is the hurricane intensity in the Saffir-Simpson wind scale and R is the distance from the site of interest to the hurricane center, normalized by the hurricane's radius of the outermost closed isobar (ROCI). ROCI is estimated from the synthetic storms' size using an empirical equation[25]. Supplementary Figure 1 shows f for multiple values of C and R. Following the procedure in Ceferino et al., 2022[25], irradiance at the site is sampled using a lognormal distribution fitted to each county's 20-year history of irradiance[32], for every two hours during the lifespan of each synthetic hurricane.

Damage to panels during storms. High hurricane winds increase the likelihood of panels' structural failure and loss of functionality. The functional form of damage likelihood, i.e., fragility function, is typically defined as a cumulative density function of the logarithm, and it uses natural hazards' intensities as input, like maximum wind for hurricanes or spectral acceleration for earthquakes. Accordingly, we utilized the following fragility function recently calibrated[29] with a ground-truth data on panel structural performance after Hurricane Irma and Maria in 2017 and Dorian in 2019[20–22]

$$q = \Phi\left(\frac{ln(W) - ln(80)}{0.32}\right) \tag{19}$$

where W (m/s) is 3-second gusts at a site. Supplementary Figure 2 shows q for multiple values of W. Damage is only caused by high-intensity hurricanes. For hurricanes reaching a category of 1, W is 42 m/s (after transforming 1-m sustained winds to 3-second gusts with an empirical formula[33]), and q is only 0.02. It takes an intensity of 4 ($W = 74$ m/s) to increase the probability of failure to 0.4. In our model F equal 1 until t_d and 0 after. If the panel is undamaged, then the time to failure $t_d = \infty$. Thus, $t = \infty$ with probability of $1 - q_{max}$, where q_{max} is the maximum q induced at the site of interest during the lifespan of the hurricane. Otherwise, if $t_d < \infty$, i.e., there is a failure.

We modeled the time to failure stochastically, with probability of failure at time t proportional to the varying values of q during the hurricane's lifespan. While high-resolution and high-fidelity structural analysis models may better capture t_d, this simplified approach accounts for the fact that it is more likely to have failures during the highest wind conditions imposed by hurricanes.

Hurricane Simulation. We used a synthetic hurricane database with 5018 landfalling storms in the United States' Atlantic Coast, and simulated 10 time series of solar generation for each storm, reaching to ~50,000 simulations. The synthetic hurricanes were generated in a previous study[30] using a statistical-deterministic tropical cyclone model. These synthetic hurricanes account for current climate conditions, representative of hurricane activity from 1980 to 2005 according to the National Center for Environmental Prediction (NCEP) reanalysis. The model that generates these storms consists of three stages: a probabilistic genesis model; a probabilistic beta-advection motion model; and a deterministic model that captures how environmental factors influence storm development and intensity.[34] The model solves the synthetic storms' tracks, maximum sustained winds, and radii of maximum winds, and we use its results at 2-hour intervals. We estimated the total wind fields with a complete wind profile model[35] and background winds.[36] According to the current hurricane occurrence rate, the total ~50,000 simulations are representative of ~15,000 years of simulation of solar generation during storms.

Results and Discussion

We studied the impact of a large number of synthetic storms[30] making landfall on the US Atlantic Coast. The storm simulations account for current climate conditions and include the assessment of the synthetic storms' tracks, sizes, and wind fields at 2-hour intervals. We determined A_c and A_d at this high temporal resolution to capture intermittency of solar generation within a day and its seasonal variability during storms, which occur at different monthly rates.[37]

To capture different risk levels, we use our probabilistic approach to estimate the return periods (RPs) for the total reduction factor, A_cA_d, as the inverse of the annual exceedance rates λ. Using the n Monte Carlo simulations, we computed the empirical estimate of this rate as

$$\hat{\lambda}(A_cA_d > x) = \frac{\sum_{i=1}^{n} 1\{A_c^i A_d^i > x\}}{T} \quad (20)$$

where x is the threshold of interest. The summation computes the number of simulations (with index i) that exceed the threshold, and T is the equivalent number of years of simulation. We followed a similar procedure to calculate the RPs for A_c and A_d.

Risk of Solar Generation in Miami-Dade. We utilized our proposed framework to first generate ~50,000 Monte Carlo simulations of the time series of P and E in Miami-Dade, Florida (Supplementary Figure 3). We characterized the occurrence of energy losses probabilistically, estimating different levels of total reduction factor, i.e., A_cA_d (Equation (3)), and their associated return periods RP (Equation (20(3)). The total reduction factor was assessed for the total harvested solar energy starting the day before hurricane landfall, i.e., $t = 0$, because important energy losses also occur when the hurricane's center is still on the ocean but nearing the coastline [25,38].

Our simulations capture how more extreme events (longer RP) trigger larger solar energy losses, i.e., large total reduction factors A_cA_d, across the wide range of return periods at landfall, and one ($t_f = 24h$), two ($t_f = 48h$) and three ($t_f = 96h$) days after (Figure 3a). We show that frequent events will induce large energy generation losses, with total reduction factors increasing sharply in the initial return period range. Miami-Dade will lose 70, 63, 52, and 40% of its solar generation, i.e., A_cA_d of 3.3, 2.7, 2.1, and 1.67, at landfall, and one, two and three days after, respectively, for hurricane emergencies happening on average every 50 years ($RP = 50$ years).

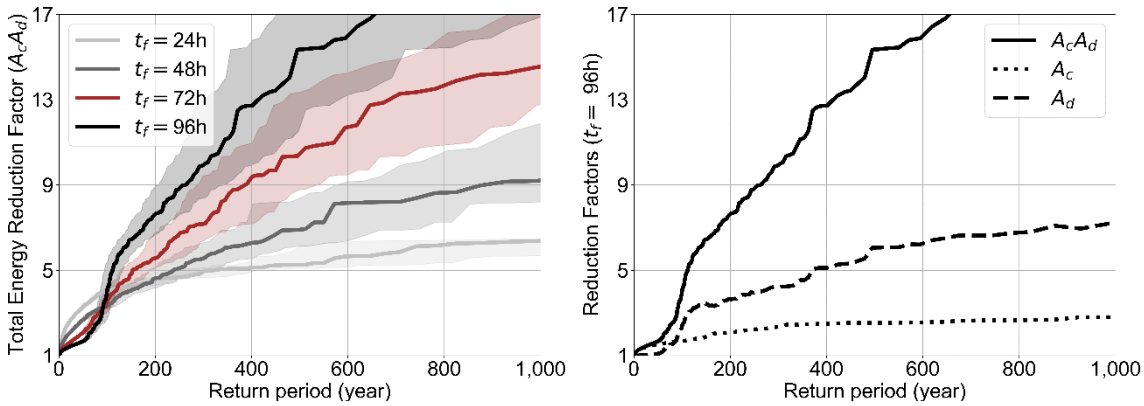

Figure 3. *Return periods for different levels of relative energy loss due to hurricanes for Miami-Dade, Florida.* ***Left:*** *The relative energy loss is depicted through total reduction factors, $A_c \times A_d$, equal to the cumulative energy harvested by the panel until landfall and one, two and three days after ($t_f = 24, 48, 72, 96h$) compared to the counterfactual event, i.e., generation in the absence of a hurricane. 95-% Confidence are estimated using χ^2 distributions for Poisson rate estimates[39] and are shown as shaded areas.* ***Right:*** *The total reduction factor is decomposed in its two factors, A_c and A_d, for cumulative energy until 72 hours after landfall ($t_f = 96h$) to highlight the contributions of cloud conditions and panel damage in the energy losses for different return periods.*

Time-variant contributions of reduction factors. We observe that the total reduction factor is bigger at landfall than three days after for the "frequent" events (Figure 3a). However, they reach similar values, A_cA_d of ~3.4 for hurricanes with RP of ~90 years. For rarer events, the order flips, and energy losses increase over time after landfall in Miami-Dade, due to the varying contributions of the factors A_c and A_d through the wide range of return periods (Figure 3b). A_c is initially bigger than A_d until they reach a similar value of 1.7 for a RP of ~90 years for $t_f = 96h$. This RP threshold coincides with the transition from increasing to decreasing values of A_cA_d as a function of t_f. Empirically, we demonstrate that this transition is dominated by the change in the energy loss mode, from predominantly transient and cloud-induced to permanent and damage-induced losses.

We also observe transient but strong cloud-induced energy losses especially for small t_f. For example, at $t_f = 6h$, i.e., 18 hours before landfall, hurricanes with RP of 200 years will trigger losses of 68% (Figure 4a), almost entirely due to the hurricane clouds ($A_c = 3.1$ and $A_d = \sim 1$). Cloud-induced losses will reach their maximum values of 77% ($A_c = 4.4$) for $24 < t_f < 36h$ (between landfall and the 12 hours after). This observation is consistent with presence of optically thick cloud structures (with high moisture levels and vertical depths) in the hurricane eyewalls[40] that will cover Miami-Dade after landfall. More frequent events can also induce large energy losses. Clouds from storms with RP of only 9 years will induce losses of 50% ($A_c = 2$) at $t_f = 6h$. These strong cloud effects are transient. Thirteen days after landfall, A_c is only 1.19, which is a modest energy loss of 11% for an extreme event with return period of 200 years (Figure 4a). Notice that in the limit, cloud-induced losses will be negligible, i.e., $A_c = 1$ (Equation (14)).

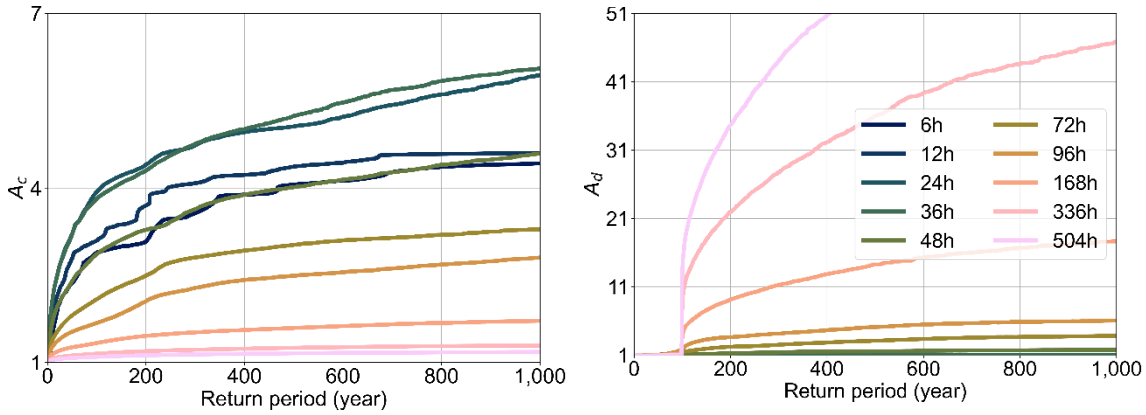

Figure 4. *Time-varying behavior of compounding factors A_c and A_d across different return periods.* ***Left:*** *Reduction factor due to cloud conditions (A_c).* ***Right:*** *Reduction factor due solar panel damage (A_d). The reduction factors are estimated for cumulative energy losses starting at 24 hours after landfall until different t_f values, i.e., the values of A_c and A_d for $t_f = 6h$ correspond to cumulative since 24 hours before landfall until 18 hours before landfall.*

Less frequent events ($RP > \sim 90$ years) can have permanent effects on energy (Figure 4b). A_d is close to 1 for $RP < \sim 90$ years for all values of t_f, and then, it grows steadily as a function of the return period given that these extreme events will induce higher solar panel damage likelihoods (Supplementary Figure 2). In contrast to A_c, A_d is close to 1 (below 1.03), i.e., no effects, until $t_f = 36h$ (12 hours after landfall) even for very extreme events with RP of 1,000 years, demonstrating that storms require additional time to be near the site and damage panels. If the panel is damaged, then energy losses will grow to infinite unless the panel is repaired or replaced (Equation (16)). Accordingly, the factor A_d becomes rapidly dominant for damaged panels. For storms with RP of 200 years, the ratio between A_d and A_c is 0.4 at $t_f = 48h$, but it increases to 1.8 only $48h$ after (Figure 4). These results demonstrate that structural reliability is critical for generation reliability during a hurricane emergency.

Storms' features driving bigger energy losses: We de-aggregated the storm simulations to assess the storm features driving large energy losses quantitatively. We analyzed the joint probability distribution of category C and distance to the site d, empirically, utilizing 500,000 Monte Carlo simulations instead of 50,000 to estimate these joint distributions more smoothly. We analyzed the drivers for energy losses of 33% and 50%, i.e., $A_c A_d$ of 1.3 (RP of 12 years) and 2 (RP of 58 years), at $t_f = 96h$ (Figure 5). The average hurricane categories that caused these losses were 3.1 and 3.6, and the average closest distances are 66 and 33 km, respectively. Hurricane cloud conditions rather than high winds drove the reduction factor of 1.3 as 88% of the events did not cause panel failure. 33% of these synthetic storms did not reach hurricane categories beyond two, and 44% were more than 50 km away, indicating that the 1.3 reduction factor can be caused by events distant from the site. For the reduction factor of 2, panels experienced failures in 69% of the simulations, indicating that significant panel damage can occur even at return periods lower than 90 years, as discussed above. Moreover, 72% of the simulations had storms with categories above three, and 90% had distances from the track to the site of 50 km or less. These results are consistent with frequent observations of hurricane's maximum winds at radii between 20 and 80 km.[41]

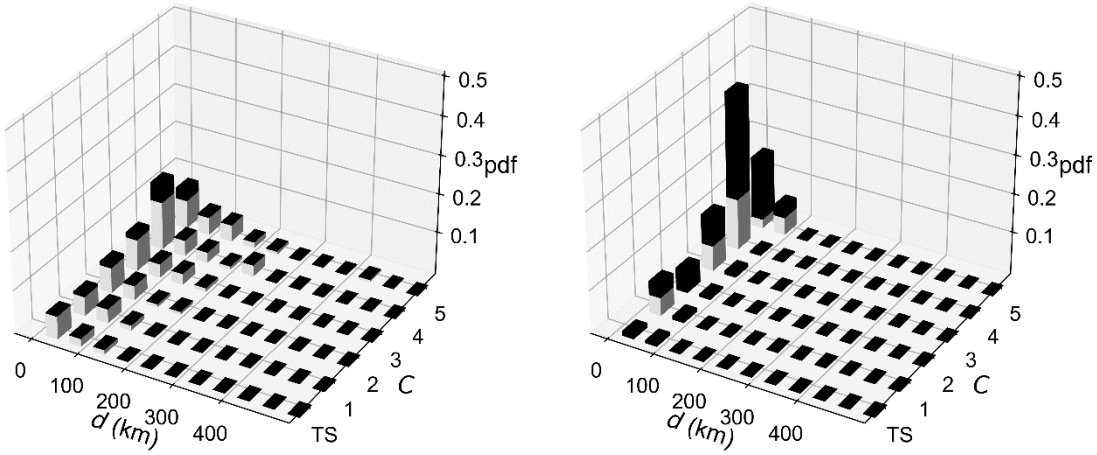

Figure 5. *Analysis of the drivers of energy capacity loss through de-aggregation of the simulations for Miami-Dade, Florida.* ***Left:*** $A_1A_2 = 1.3$ $(A_c = 1.29, A_d = 1.01,\ RP = 12\ years)$. ***Right:*** $A_1A_2 = 2$ $(A_c = 1.59, A_d = 1.26, RP = 58\ years)$. *The plots show histograms of the storms' features that triggered generation losses of 33 and 50%, respectively, or lower. The black portion of the plot represents losses associated to structural failures and the white ones represent losses due to hurricane clouds. The plots highlight that larger capacity losses are driven by structural failures rather than hurricane cloud conditions.*

Annual rates of panel failure in Central and Eastern United States: We extended the analysis to the entire Central and Eastern United States and generated 50,000 Monte Carlo simulations for their 2694 counties in 38 states. We first focused on simulations of structural damage to assess the spatial distribution of RP and reliability indexes of panel failures. As defined in the ASCE7-16[42], the structural index β is estimated as the cumulative distribution function for a standard normal random variable evaluated on the probability of infrastructure survival (the complementary of failure) in 50 years. Thus,

$$\beta = \Phi^{-1}\left(\exp\left(-50\lambda_f\right)\right) \tag{21}$$

where λ_f is the annual probability of panel failure, equal to the inverse of RP. We estimated λ_f empirically from the 50,000 Monte Carlo simulations in the 38 states, as in a Maximum Likelihood Estimation of a Poisson distribution's rate, and then computed RP (Figure 6a) and β (Figure 6b). We show that Florida and Louisiana face the highest failure risks due to hurricanes, with average RP of 174 years and 265 years across all their counties. 55% and 41% of the counties in Florida and Louisiana have RP of panel failure below 200 years. Our results also show that Texas, Mississippi, Alabama, Georgia, and Southern and Northern Carolina also have high risks, where installed solar panels will experience failures with RP below 600 years in 19%, 22%, 19%, 26%, 24%, and 12% of their counties, respectively.

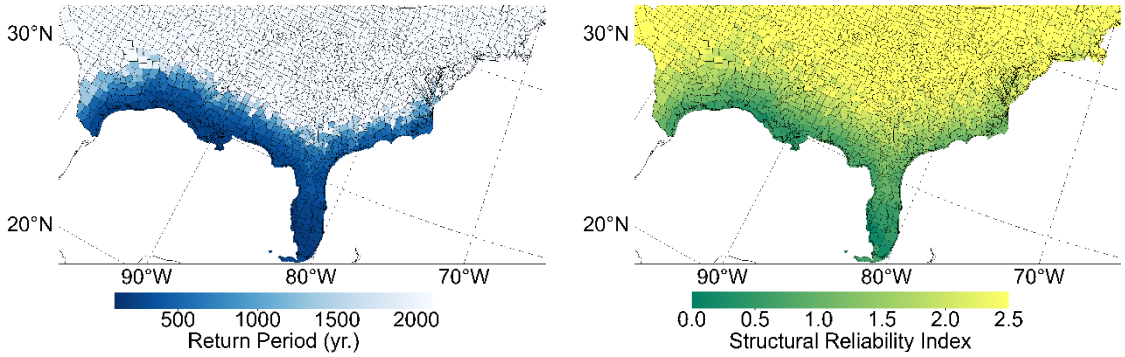

Figure 6. *Spatial distribution of return period of structural failure and reliability index for solar panels located on different counties in Central and Eastern United States.* ***Left:*** *Return Period.* ***Right:*** *Structural Reliability Index. The plot highlights that Southern United States have significantly lower reliability than threshold.*

Using results from a recent reliability study that assessed wind loads and capacities according to ASCE7-16[43], we estimated that a structure well designed for Risk Category II (winds with a 700-year return period) should have a β at or above 2.3.[42] For the Risk category I (winds with a 300-year return period), the lowest design standard in ASCE7-16, a well-designed structure should achieve a β value at or above 1.9.[29,42,43] Our results indicate that the panel installations in Texas, Louisiana, Mississippi, Alabama, Florida, Georgia, and Southern and Northern Carolina have β values below 1.9 in 62% of their counties. Thus, these results reveal extensive structural vulnerabilities and highlight that panels are below all ASCE7-16 standards for resilience in large regions in Southern US (Figure 6b).

Spatial Distribution of Solar Generation Losses in Central and Eastern United States: Next, we assessed generation during storms in Central and Eastern US. We generated 50,000 Monte Carlo Simulations of the time series of P and E for panels in the 2694 counties' centroids (see example in Texas and North Carolina in Supplementary Figure 4). Similar to the analysis in Miami-Dade, we determined the reduction factors A_c and A_d at different return periods. We focused on cumulative energy at $t_f = 24\ h$ (Figure 7), $48\ h$ (Supplementary Figure 5), $72\ h$ (Figure 8) and $96\ h$ (Supplementary Figure 6).

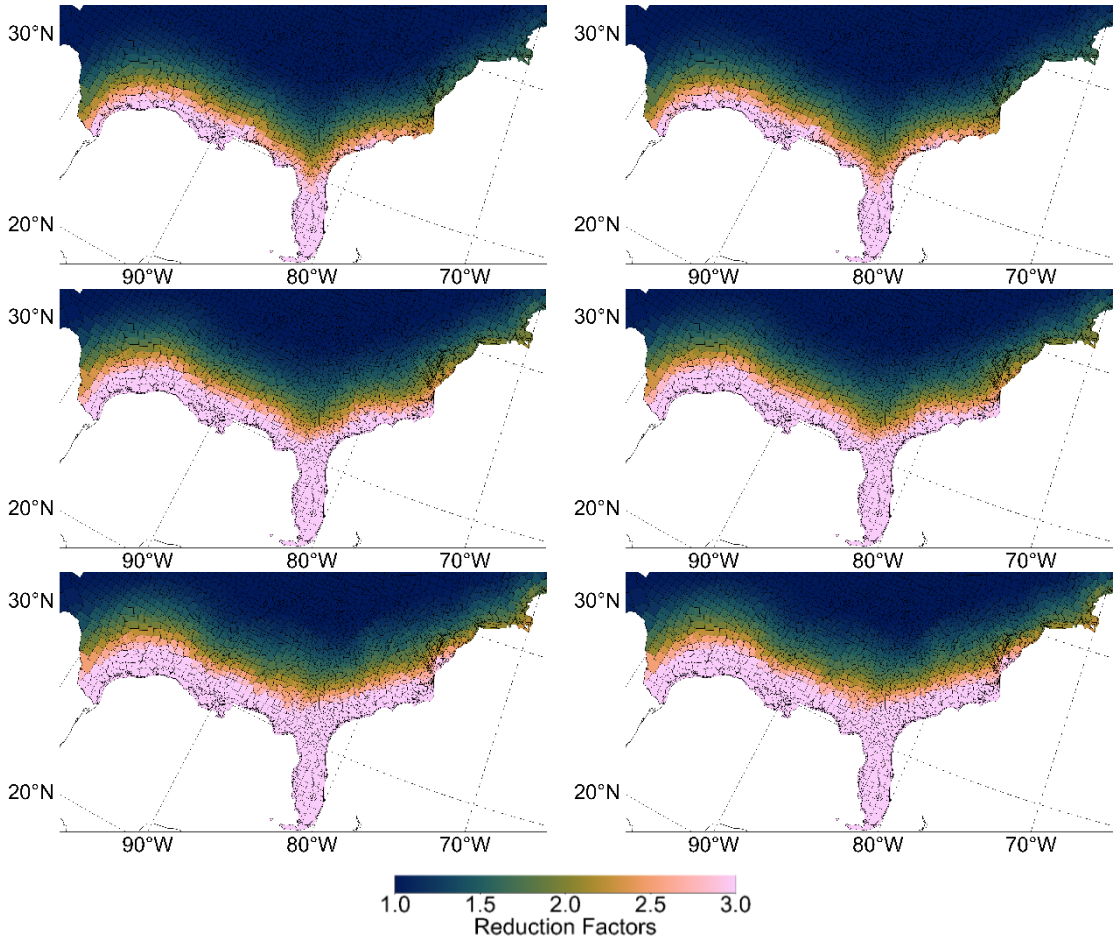

Figure 7. *Spatial distribution of energy generation losses for uniform risk targets (associated to return periods) in Central and Eastern United States and the compounding factors for energy losses at landfall ($t_f = 24h$).* ***Upper Left:*** *A_c for events with 100-years of return period.* ***Upper Right:*** *$A_c A_d$ for events with 100-years of return period.* ***Middle Left:*** *A_c for events with 300-years of return period.* ***Middle Right:*** *$A_c A_d$ for events with 300-years of return period.* ***Lower Left:*** *A_c for events with 700-years of return period.* ***Lower Right:*** *$A_c A_d$ for events with 700-years of return period.*

The spatial distribution of A_c at $t_f = 24h$ reveals that hurricane clouds will induce significant energy losses at landfall even at tens of kilometers away from the Southern and Eastern coastline (Figure 7). For RP of 100 years, Florida and Louisiana will only harvest 32% ($A_c = 3.13$) and 65% ($A_c = 1.54$) of their regular solar energy on average across all their counties, with hardest-hit counties generating only at 23% ($A_c = 4.27$) and 27% ($A_c = 3.65$), respectively. More extreme events will increase the intensity and the spatial extent of high energy losses. For RP of 300 years, Florida and Louisiana will only harvest 21% ($A_c = 4.80$) and 50% ($A_c = 2.01$) on average across all their counties. For RP of 700 years, they will only harvest 25% ($A_c = 4$) and 54% ($A_c = 1.84$), with hardest-hit counties generating only at 17% ($A_c = 5.83$) and 18% ($A_c = 5.46$) of regular capacity, respectively. All Southern and Central counties near the coastline up to the ones in Virginia, Maryland and Delaware will have reduced generation equal or below 33% due to the storm clouds ($A_c > \sim 3$).

Our results show that compounding effects will be critical only after $t_f = 24h$, i.e., at landfall. Before, $A_c A_d$ is almost equivalent to A_c across the different levels of storms' return periods for all counties (Figure 7). However, at $t_f = 72h$ (two days after landfall), we start observing important contributions of solar damage to the energy losses (Figure 8). At this time, Florida and Louisiana already experience 26% and 15% less energy losses than at landfall, thanks to the recovery of regular

irradiance levels after the hurricane leaves, and damage-induced losses will start dominating the total energy losses. In counties in the coastline, this transition can happen as early as 24 hours after landfall (Supplementary Figure 4). For RP of 300 years, A_d across all of Florida and Louisiana's counties are 2.03 and 1.13 at $t_f = 72h$ (two days after landfall), inducing energy losses that are 25% and 9% higher than those when panels do not fail, respectively. For RP of 700 years, the compounding effect of damage becomes stronger since A_d increases to 3.48 and 1.39 for Florida and Louisiana, respectively, inducing 38 and 25% higher losses, which will become even stronger for longer t_f (Supplementary Figure 5).

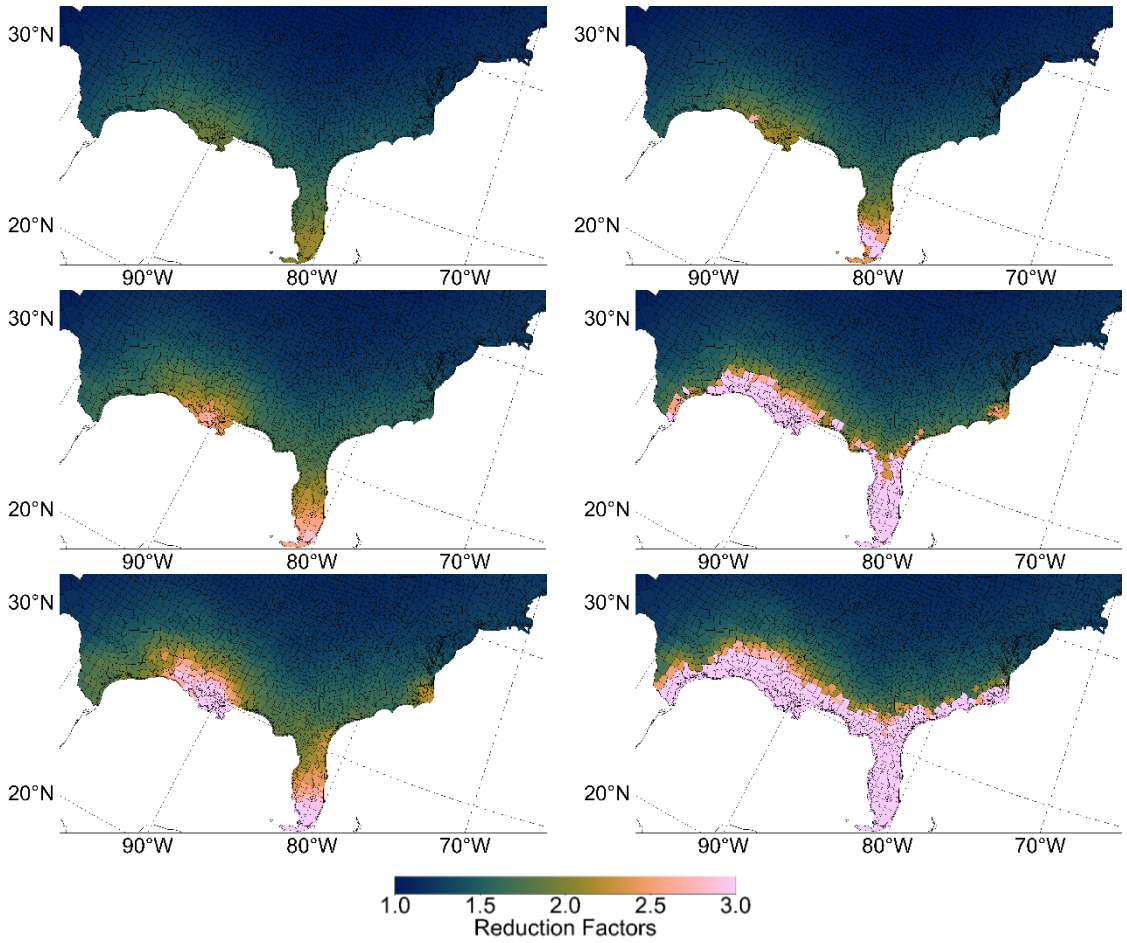

Figure 8. *Spatial distribution of energy generation losses for uniform risk targets (associated to return periods) in Central and Eastern United States and the compounding factors for energy losses 48 hours after landfall ($t_f = 72h$).* ***Upper Left:*** *A_c for events with 100-years of return period.* ***Upper Right:*** *$A_c A_d$ for events with 100-years of return period.* ***Middle Left:*** *A_c for events with 300-years of return period.* ***Middle Right:*** *$A_c A_d$ for events with 300-years of return period.* ***Lower Left:*** *A_c for events with 700-years of return period.* ***Lower Right:*** *$A_c A_d$ for events with 700-years of return period.*

Discussion. In sum, our results show that hurricane's impacts on solar generation are significant, compounding and strikingly disproportional in the United States. Clouds can induce losses above 66% in extensive regions in Southern and Eastern United States (see RP of 100 years in Figure 7), but fortunately, these effects are only transient. In contrast, damage to solar panels will induce more acute and permanent energy losses but fortunately in smaller extents (see counties with highest risk of panel failure in Figure 6). When these two effects are compounded, solar generation risk will induce large energy losses throughout the entire hurricane emergency.

A direct implication of this study is that the naïve adoption of panels in the current conditions will create electricity generating infrastructure with high risks, especially in Louisiana and Florida, which have experienced massive hurricane outages in the last few years.[2,44,45] Building stronger panels can help prevent panel damage, i.e., making $A_d = 1$. Thus, this paper advocates installing stronger panels, at least up to the ASCE-7 standards for infrastructure with risk category I. Existing studies point out that cheap solutions can increase the performance of solar installation's structural system, e.g., torque check on bolts.[20,22] If panels do not fail, all solar energy reductions (A_c) will be driven by hurricane clouds only, making solar energy losses only transient.

These results underscore that massive investments in resilience and clean energy in power infrastructure will pay off if their deployment is risk-informed. Placing panels on coastlines in the Southern or Eastern US can make the grid lose (sometimes permanently) solar generation during hurricane emergencies (Figure 7 and Figure 8). Power system models can optimize the deployment of new solar farms, maximizing profits for regulators, power utility companies, and consumers. But they should also assess resilience to consider the trade-off between costs and risks, especially in Florida and Louisiana, where generation potential is high, but risks are also high.

Additionally, for communities exposed to high risks, like those in Miami-Dade or New Orleans (Louisiana) installing decentralized resources, such as rooftop panels and behind-the-meter batteries must account for the potential high reduction in energy generation. Even if they have continuous power supply even in case of a main grid's outage, they should still plan for only using necessary building functions in a hurricane emergency, e.g., refrigeration for food or even cooling especially if heatwaves follow storms.[46]

This paper also advocates risk-informed utility companies' contingency planning during extreme events. We provide a framework to account for these losses quantitatively so that utility companies can plan for offsetting the large losses in solar generation from other sources. In the context of disaster, additional difficulties might arise from failures in transmission lines that prevent the use of other functional electricity sources. Thus, it is critical for utility companies to install robust generating infrastructure to ensure the resilience of our future grids, especially since global warming is projected to intensify hurricanes in the future climate.[47]

Acknowledgments

We acknowledge the financial support by the Tandon School of Engineering at the New York University and the Andlinger Center for Energy and the Environment at Princeton University. Additionally, this research was also supported by the NSF Grant 1652448. The authors are grateful for their generous support. We also thank Dr. Dazhi Xi, from Princeton University, for his help in generating the wind fields and Dr. Charalampos Avraam, from New York University, for his insightful comments and revisions to our study's contributions for power systems resilience.

References

1. Wang, Z. *et al.* Monitoring Disaster-Related Power Outages Using Nasa Black Marble Nighttime Light Product. *ISPRS - International Archives of the Photogrammetry, Remote Sensing and Spatial Information Sciences* **XLII–3**, 1853–1856 (2018).
2. Boyle, L. Louisiana's power grid took a bigger blow from Hurricane Ida than any other storm in history. *Independent* https://www.independent.co.uk/climate-change/news/hurricane-ida-power-grid-louisiana-b1915145.html (2021).
3. Swiss Re Institute. *Natural catastrophes in 2021 : the floodgates are open*. (2022).
4. The White House. President Biden's Bipartisan Infrastructure Law. https://www.whitehouse.gov/bipartisan-infrastructure-law/#:~:text=The Bipartisan Infrastructure Law will deliver %2465 billion to help,investment in broadband infrastructure deployment. (2022).
5. Department of Energy. DOE Optimizes Structure to Implement $62 Billion in Clean Energy Investments From Bipartisan Infrastructure Law. https://www.energy.gov/articles/doe-optimizes-structure-implement-62-billion-clean-energy-investments-bipartisan (2022).
6. US Energy Information Administration. *Annual Energy Outlook 2022*. https://www.eia.gov/outlooks/aeo/data/browser/#/?id=16-AEO2022&region=0-0&cases=ref2022&start=2020&end=2050&f=A&linechart=ref2022-d011222a.4-16-AEO2022&sourcekey=0; in GW (2022).
7. Patel, S., Ceferino, L., Liu, C., Kiremidjian, A. & Rajagopal, R. The disaster resilience value of shared rooftop solar systems in residential communities. *Earthquake Spectra* 1–24 (2021) doi:10.1177/87552930211020020.
8. Ceferino, L. *et al.* Earthquake resilience of distributed energy resources. in *17th World Conference on Earthquake Engineering* (2020).
9. Anderson, K. *et al.* Quantifying and monetizing renewable energy resiliency. *Sustainability (Switzerland)* **10**, 1–13 (2018).
10. Laws, N. D., Anderson, K., DiOrio, N. A., Li, X. & McLaren, J. Impacts of valuing resilience on cost-optimal PV and storage systems for commercial buildings. *Renew Energy* **127**, 896–909 (2018).
11. Colson, C. M., Nehrir, M. H. & Gunderson, R. W. Distributed multi-agent microgrids: A decentralized approach to resilient power system self-healing. *Proceedings - ISRCS 2011: 4th International Symposium on Resilient Control Systems* 83–88 (2011) doi:10.1109/ISRCS.2011.6016094.
12. Talebiyan, H. & Duenas-Osorio, L. Decentralized Decision Making for the Restoration of Interdependent Networks. *ASCE ASME J Risk Uncertain Eng Syst A Civ Eng* **6**, 04020012 (2020).
13. Ouyang, M., Dueñas-Osorio, L. & Min, X. A three-stage resilience analysis framework for urban infrastructure systems. *Structural Safety* **36–37**, 23–31 (2012).
14. Winkler, J., Dueñas-Osorio, L., Stein, R. & Subramanian, D. Performance assessment of topologically diverse power systems subjected to hurricane events. *Reliab Eng Syst Saf* **95**, 323–336 (2010).

15. Nateghi, R., Guikema, S. & Quiring, S. M. Power Outage Estimation for Tropical Cyclones: Improved Accuracy with Simpler Models. *Risk Analysis* **34**, 1069–1078 (2014).
16. Bennett, J. A. *et al.* Extending energy system modelling to include extreme weather risks and application to hurricane events in Puerto Rico. *Nat Energy* **6**, (2021).
17. Shashaani, S., Guikema, S. D., Zhai, C., Pino, J. v. & Quiring, S. M. Multi-Stage Prediction for Zero-Inflated Hurricane Induced Power Outages. *IEEE Access* **6**, 62432–62449 (2018).
18. Han, S. R., Guikema, S. D. & Quiring, S. M. Improving the predictive accuracy of hurricane power outage forecasts using generalized additive models. *Risk Analysis* **29**, 1443–1453 (2009).
19. Guikema, S. D., Quiring, S. M. & Han, S. R. Prestorm Estimation of Hurricane Damage to Electric Power Distribution Systems. *Risk Analysis* **30**, 1744–1752 (2010).
20. Burgess, C. & Goodman, J. Solar Under Storm. Select Best Practices for Resilient Ground-Mount PV Systems with Hurricane Exposure. (2018).
21. Stone, L., Burgess, C. & Locke, J. *Solar Under the Storm for Policymakers: Select Best Practices for Resilient Photovoltaic Systems for Small Island Developing States*. www.rmi.org/insight/solar- under-storm-for-policymakers. (2020).
22. Burgess, C., Detweiler, S., Needham, C. & Oudheusden, F. *Solar Under Storm Part II: Select Best Practices for Resilient Roof-Mount PV Systems with Hurricane Exposure*. www.clintonfoundation.org/Solar- (2020).
23. Liu, Y. & Zhong, J. Risk assessment of power systems under extreme weather conditions - A review. *2017 IEEE Manchester PowerTech, Powertech 2017* 22–27 (2017) doi:10.1109/PTC.2017.7981141.
24. Cole, W., Greer, D. & Lamb, K. The potential for using local PV to meet critical loads during hurricanes. *Solar Energy* **205**, 37–43 (2020).
25. Ceferino, L., Lin, N. & Xi, D. Stochastic modeling of solar irradiance during hurricanes. *Stochastic Environmental Research and Risk Assessment* (2022) doi:10.1007/s00477-021-02154-2.
26. Vickery, P. J., Wadhera, D., Twisdale, L. A. & Lavelle, F. M. U.S. Hurricane Wind Speed Risk and Uncertainty. *Journal of Structural Engineering* **135**, 301–320 (2009).
27. Vickery, P. J., Masters, F. J., Powell, M. D. & Wadhera, D. Hurricane hazard modeling: The past, present, and future. *Journal of Wind Engineering and Industrial Aerodynamics* **97**, 392–405 (2009).
28. Mitsova, D., Escaleras, M., Sapat, A., Esnard, A. M. & Lamadrid, A. J. The effects of infrastructure service disruptions and socio-economic vulnerability on Hurricane recovery. *Sustainability* **11**, 1–16 (2019).
29. Ceferino, L., Lin, N. & Xi, D. Bayesian Updating of Solar Panel Fragility Curves and Implications of Higher Panel Strength for Solar Generation Resilience. *Preprint* (2022) doi:10.31224/osf.io/dv7s3.
30. Marsooli, R., Lin, N., Emanuel, K. & Feng, K. Climate change exacerbates hurricane flood hazards along US Atlantic and Gulf Coasts in spatially varying patterns. *Nat Commun* **10**, 1–9 (2019).

31. Landsea, C. W. & Franklin, J. L. Atlantic hurricane database uncertainty and presentation of a new database format. *Mon Weather Rev* **141**, 3576–3592 (2013).
32. Sengupta, M. *et al.* The National Solar Radiation Data Base (NSRDB). *Renewable and Sustainable Energy Reviews* **89**, 51–60 (2018).
33. Vickery, P. & Skerlj, P. Hurricane Gust Factors Revisited. *Journal of Structural Engineering* **131**, 825–832 (2005).
34. Emanuel, K., Sundararajan, R. & Williams, J. Hurricanes and Global Warming: Results from Downscaling IPCC AR4 Simulations. *Bull Am Meteorol Soc* **89**, 347–368 (2008).
35. Chavas, D. R., Lin, N. & Emanuel, K. A model for the complete radial structure of the tropical cyclone wind field. Part I: Comparison with observed structure. *J Atmos Sci* **72**, 3647–3662 (2015).
36. Lin, N. & Chavas, D. On hurricane parametric wind and applications in storm surge modeling. *Journal of Geophysical Research Atmospheres* **117**, 1–19 (2012).
37. Emanuel, K. Climate and tropical cyclone activity: A new model downscaling approach. *J Clim* **19**, 4797–4802 (2006).
38. Cole, W., Greer, D. & Lamb, K. The potential for using local PV to meet critical loads during hurricanes. *Solar Energy* **205**, 37–43 (2020).
39. Ulm, K. Simple method to calculate the confidence interval of a standardized mortality ratio (SMR). *Am J Epidemiol* **131**, 373–375 (1990).
40. John, J., Shukla, B. P., Gajjar, P. N. & Sathiyamoorthy, V. Study of satellite-derived cloud microphysical parameters for tropical cyclones over the North Indian Ocean (2010–2013). *Theor Appl Climatol* **139**, 1163–1173 (2020).
41. Wang, Y. & Rosowsky, D. v. Joint distribution model for prediction of hurricane wind speed and size. *Structural Safety* **35**, 40–51 (2012).
42. American Society of Civil Engineers (ASCE). *Minimum Design Loads and Buildings and Other Structures (ASCE/SEI 7-16)*. (2017).
43. McAllister, T. P., Wang, N. & Ellingwood, B. R. Risk-Informed Mean Recurrence Intervals for Updated Wind Maps in ASCE 7-16. *Journal of Structural Engineering* **144**, 06018001 (2018).
44. Esnard, D. M. A. Socioeconomic vulnerability and electric power restoration timelines in Florida : the case of Hurricane Irma. *Natural Hazards* **94**, 689–709 (2018).
45. Prevatt, D. *et al. StEER: Hurricane Ida Joint Preliminary Virtual Reconnaissance Report - Early Access Reconnaissance Report (PVRR-EARR)*. (2021) doi:10.17603/ds2-w6km-fe51.
46. Feng, K., Min, O. & Lin, N. The hurricane-blackout-heatwave compound hazard risk and resilience in a changing climate. (2021).
47. Knutson, T. *et al.* Tropical cyclones and climate change assessment part II: Projected response to anthropogenic warming. *Bull Am Meteorol Soc* **101**, E303–E322 (2020).